Electronic Supplementary Material (ESI) for Journal of Materials Chemistry A.

Restraining the polarization increase of Ni-rich and low-Co cathodes upon cycling by Al-doping

Chunfang Zhang,[a] Jiajia Wan,[b] Yixiao Li,[b] Shiyao Zheng,[c] Ke Zhou,[b] Donghao Wang,[a] Danfeng Wang,[b] Chaoyu Hong,[b] Zhengliang Gong,*[a] and Yong Yang,*[ab]

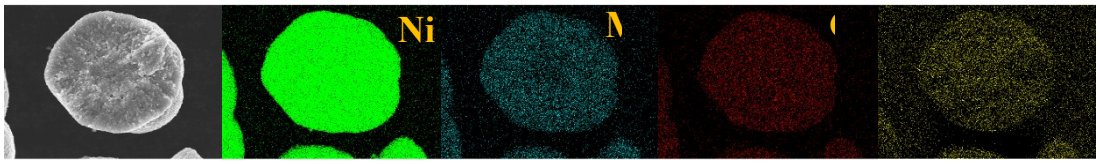

Fig. S1 Cross-sectional elemental mapping of NCMA92.

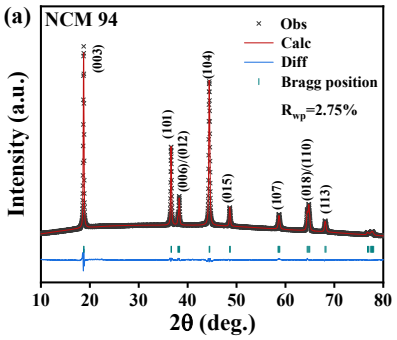

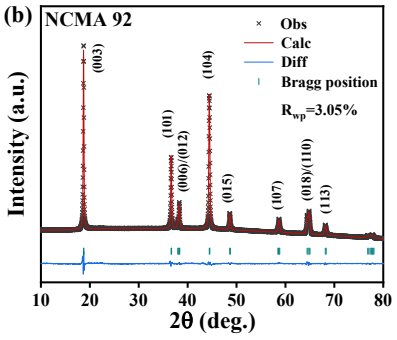

(c)

Site	X	y	z	occupancy
Li1	0.0000	0.0000	0.5000	0.9746
Ni1	0.0000	0.0000	0.0000	0.9146
Li2	0.0000	0.0000	0.0000	0.0254
Ni2	0.0000	0.0000	0.5000	0.0254
Co1	0.0000	0.0000	0.0000	0.0300
Mn1	0.0000	0.0000	0.0000	0.0300
O1	0.0000	0.0000	0.255(1)	1.0000

(d)

Site	x	Y	z	occupancy
Li1	0.0000	0.0000	0.5000	0.9761
Ni1	0.0000	0.0000	0.0000	0.8961
Li2	0.0000	0.0000	0.0000	0.0239
Ni2	0.0000	0.0000	0.5000	0.0239
Co1	0.0000	0.0000	0.0000	0.0300
Mn1	0.0000	0.0000	0.0000	0.0300
Al1	0.0000	0.0000	0.0000	0.0200
O1	0.0000	0.0000	0.256(2)	1.0000

Fig. S2 The Rietveld refinement of X-ray diffraction patterns: (a) NCM 94, (b) NCMA 92. Corresponding refined atom occupation: (c) NCM94 and (d) NCMA 92.

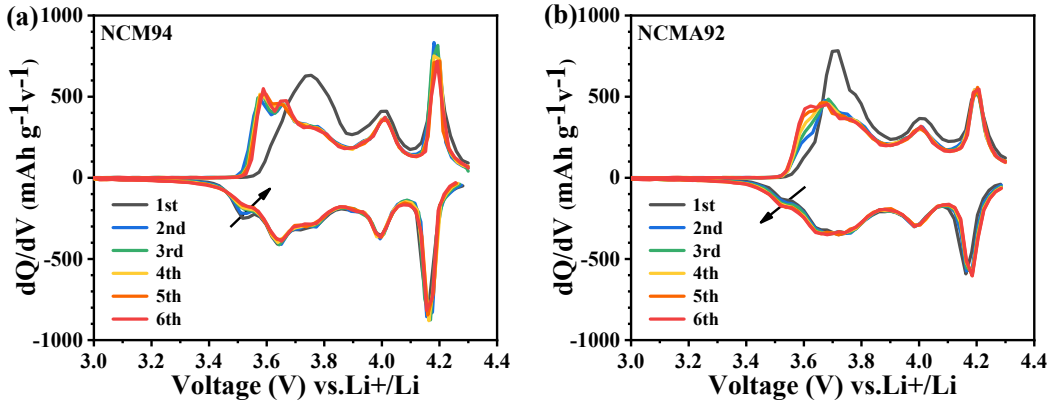

Fig. S3 Differential capacity profiles (dQ dV^{-1}) from 1st to 6th cycle at 0.1C rate: (a) NCM 94 and (b) NCMA 92.

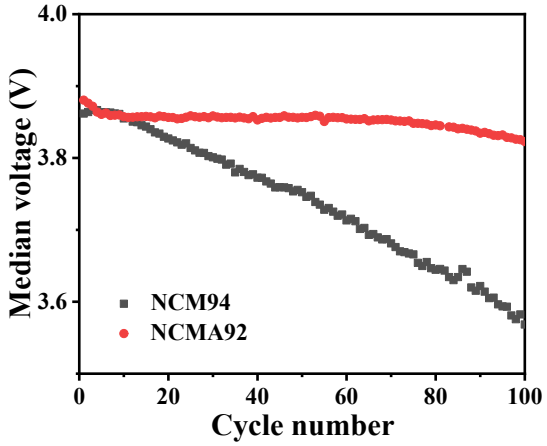

Fig. S4 Discharge median voltage as a function of cycle number during cycling at 0.5C.

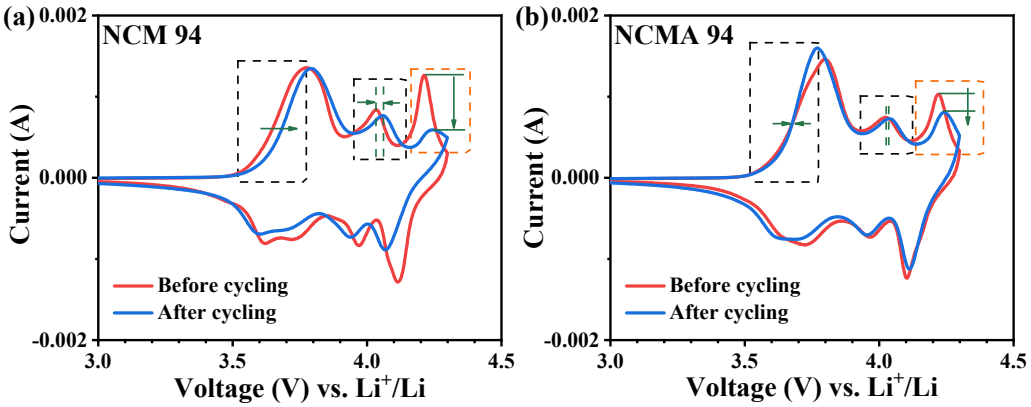

Fig. S5 Cyclic voltammogram of (a) NCM 94 and (b) NCMA92 in the potential range of 2.7-4.3 V versus Li^+/Li at 10 μV/s, which are performed before and after 50 cycles (at a 0.5C rate).

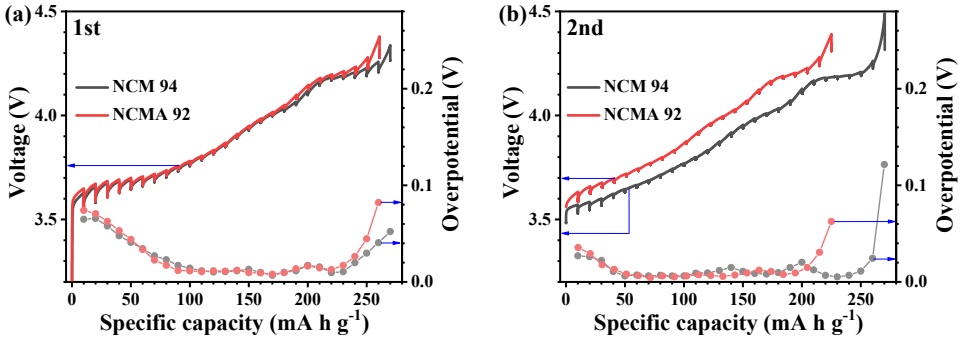

Fig. S6 GITT test results (line chart) during (a) the first charging and (b) the second charging and the corresponding voltage drop at rest (dot chart). Galvanostatic current pulses are applied with magnitudes of 20 mA g^{-1} for 30 min, followed by a 3h rest period.

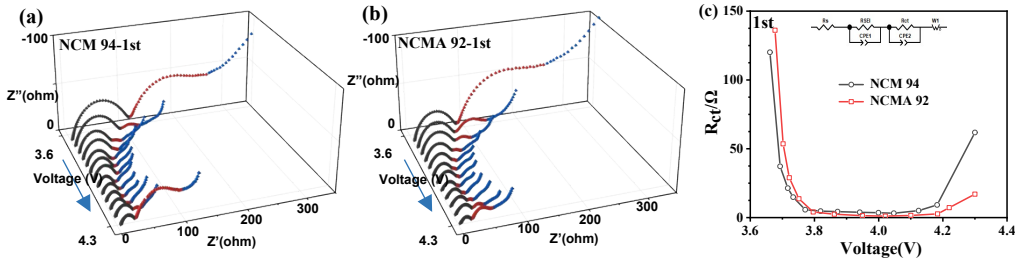

Fig. S7 Nyquist plots showing the impedance evolution during the charging process of the first cycle: (a) NCM 94 and (b) NCMA 92. (c) The corresponding fitting results of R_{ct}.

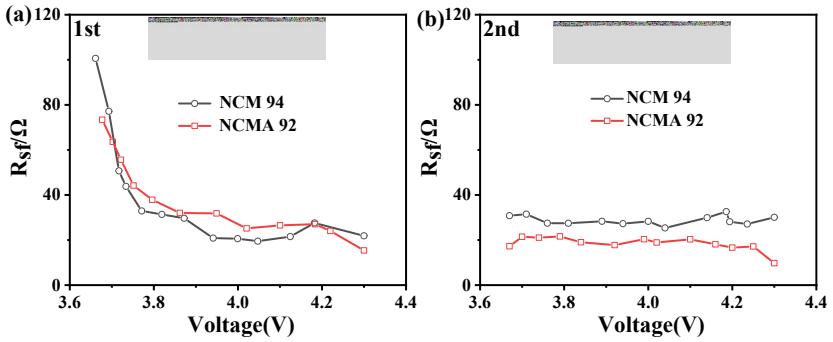

Fig. S8 The fitting results of R_f during charging of (a) the first cycle and (b) the second cycle. The corresponding Nyquist plots are shown in Fig. S5 and Fig. 8.

Table S1. Chemical compositions of Ni, Co, Mn, and Al for the NCM94 and NCMA92 cathodes measured by ICP-OES.

Sample	Value	Atomic Ratio			
		Ni	Co	Mn	Al
NCM94	Design	0.94	0.03	0.03	0
	Measurement	0.939	0.029	0.032	0
NCMA92	Design	0.92	0.03	0.03	0.02
	Measurement	0.919	0.030	0.030	0.021

Table S2. Lattice parameters of the NCM94 and NCMA92 cathodes are obtained through GSAS.

Samples	R_{wp}	R_p	a (Å)	c (Å)	V (Å^3)	Ni in Li site
NCM94	2.75%	1.72%	2.8760	14.1891	101.636	2.54%
NCMA92	3.05%	1.93%	2.8746	14.1994	101.615	2.39%

Table S3. The surface-film resistances (R_{sf}) and the charge-transfer resistance (R_{ct}) from EIS tests.

Sample	Resistance	1st	25th	50th	75th	100th
NCM94	R_{sf}/Ω	28.30	10.8	13.86	11.63	11.35
	R_{ct}/Ω	8.10	22.82	114.20	170.60	255.80
NCMA92	R_{sf}/Ω	23.92	5 .67	6.635	6.78	5.11
	R_{ct}/Ω	1.33	12.62	11.00	27.25	47.97